Journal of Colloid and Interface Science 414 (2014) 9–13

Contents lists available at ScienceDirect

Journal of Colloid and Interface Science

www.elsevier.com/locate/jcis

Slip flow of diverse liquids on robust superomniphobic surfaces

Yang Wu [a,c], Meirong Cai [a], Zhenquan Li [b], Xinwang Song [b], Hongyan Wang [b], Xiaowei Pei [a,b,c,*], Feng Zhou [a,*]

[a] State Key Laboratory of Solid Lubrication, Lanzhou Institute of Chemical Physics, Chinese Academy of Sciences, Lanzhou 730000, China
[b] Geology Institute of Shengli Oilfield, Dongying 257015, China
[c] University of Chinese Academy of Science, Beijing 100039, China

ARTICLE INFO

Article history:
Received 16 June 2013
Accepted 23 September 2013
Available online 5 October 2013

Keywords:
Slip length
Superomniphobic surface
Drag reduction
Liquids

ABSTRACT

Water slips exist over superhydrophobic solid surfaces, but the slip flow of diverse liquids on a single surface has not been deliberately studied to date. Here, we report the slip flow behavior of a variety of liquids with different surface tensions and viscosities on a robust omniphobic surface. This surface displayed a dramatic slippage effect and thus a high drag reduction efficiency of approximately 10–20% for all liquids, depending on both liquid viscosity and surface energy. The observed liquid slip was attributed to the surface dual micro/nanostructure and the low-surface-energy coating.

1. Introduction

The nature of the boundary slip of liquid past a solid surface has been actively studied because of the emergence of microfluidics and nanofluidics [1–3]. The miniaturization of devices has raised numerous problems. For instance, the rapidly increased surface-to-volume ratio increases the fluid resistance, which could lead to flow rate reduction, over-pressure, device over-heating, and surface wear. The first step to address these issues was to reduce the hydraulic resistance. Several drag reduction techniques on macroscopic scale have been reported, such as surface riblets [4], compliant coatings [5], diluted polymer solution [6,7], air bubbles [8], and superhydrophobic surfaces [9,10]. Superhydrophobic surfaces have promising application potentials for drag reduction in microfluidics. Likewise, the design of surfaces that repel to various transported liquids is well studied in the past several years and many attempts have been made to construct robust omniphobic surfaces [11–13].

It is well studied that boundary slip is often characterized by slip length (L_s), which is defined as the distance between the surface and the point inside the surface at which the extrapolated velocity of the fluid equals to zero [14]. By this definition, the slip length can be expressed as follows:

$$v_s = L_s \frac{\partial v}{\partial H}, \tag{1}$$

where v_s is the slip velocity of a fluid on a solid surface, L_s is the slip length, and $\frac{\partial v}{\partial H}$ is the velocity gradient in a direction normal to the surface. The gas at the solid–liquid interface has been attributed to the boundary slip [15,16] because of the replacement of the liquid–solid shear by the liquid–air shear at the interface. For Couette flow, an air layer separates the liquid from the solid wall, which leads to the flow over the solid surface with little friction. The resulting L_s that is caused by the pure air layer with a thickness h can be expressed as follows [17]:

$$L_s = h\left(\frac{\mu_l}{\mu_a} - 1\right), \tag{2}$$

where μ_l and μ_a are the viscosities of liquid and air, respectively. From the formulation, L_s is affected by the viscosities of the liquid and the air above the surface. Thus, the air fraction on the superhydrophobic surface would influence fluid slippage. Lee and Kim [18] reported a dual-structure Si surface could achieve 98% gas fraction in its micro/nanostructure. The measured maximum slip length of ~400 μm was much larger than that of the micro-smooth hydrophobic Si surface. Zhou [19] performed a series of rheological experiments on superhydrophobic surfaces coated with carbon nanotube (CNT) forests to reveal the effects of the surface morphology on the slip length. Belyaev [20] analyzed patterned surfaces with large effective slip lengths using hydrophobic disk approach. The results showed that the boundary slip and drag reduction were especially pronounced in a small gap and depended strongly on the fraction of the gas phase and the local slip length at the gas area.

* Corresponding authors. Address: State Key Laboratory of Solid Lubrication, Lanzhou Institute of Chemical Physics, Chinese Academy of Sciences, Lanzhou 730000, China (X. Pei). Fax: +86 931 8277088.
E-mail addresses: peixw@licp.cas.cn (X. Pei), zhouf@licp.cas.cn (F. Zhou).

0021-9797/$ - see front matter © 2013 Elsevier Inc. All rights reserved.
http://dx.doi.org/10.1016/j.jcis.2013.09.041

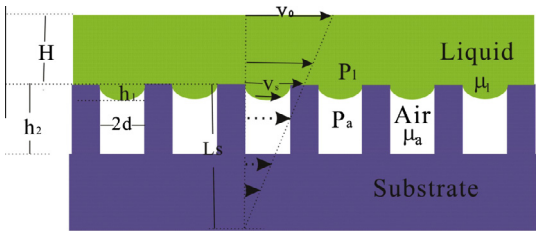

Fig. 1. Schematic of the large slip by a superhydro/olephobic surface in Couette flow.

Most of the previous studies [21–24] have used water as the detecting liquid because of its high surface tension. Reports on the flow slip of liquids with lower surface tension are rare because the surface wettability may be easily changed due to the metastability of most superhydro/oleophobic surfaces and the occurrence of wetting transitions during tests. To construct a robust omniphobic surface with conical posts, the height b and the cone angle 2α of posts were considered [25]. Based on the Laplace–Young equation, the postheight b and interpost pitch d can be obtained from the simple geometrical calculations using the following equation:

$$b > \frac{1-\sin(\theta_A-\alpha)}{\sqrt{2}|\cos(\theta_A-\alpha)|}, \tag{3}$$

and

$$d < 2\sqrt{2}\gamma\frac{|\cos(\theta_A-\alpha)|}{\Delta p}, \tag{4}$$

where Δp is the difference of the liquid pressure and the air pressure, γ is the surface tension of the liquid, and θ_A is the contact angle. The distance and height of the two conical posts have to meet the above mentioned criteria to support the liquid meniscus, which should not touch the bottom surface between the posts. That is, the sagging height of the detecting liquid (h_1) must be less than the maximum pore depth (h_2), as shown in Fig. 1, so as to the boundary slip occurs. In this article, seven liquids with surface tension in the range of 72.1–26.8 mN m^{-1} were selected as the detecting liquids to determine the boundary slip on our test surface, which was measured using a rheometer. Base on experimental results, the dependence of the slippage effect on the surface tension and the viscosity of liquids was discussed. The stable oleophobic performance of anodized aluminum that owned obvious drag-reducing property may apply to crude oil transportation or microfluidic devices.

2. Materials and methods

2.1. Materials

Aluminum (99.99% purity) sheets were purchased from Grikin Advanced Materials Co., Ltd. (China). 1H, 1H, 2H, 2H-perfluorooctyltrichlorosilane were purchased from Aldrich (USA). Diiodomethane (A.R. Tianjin, China), B-104(1-methyl-3-butylimidazolium tetrafluoroborate ionic liquid) and PAO-2, poly(α-olefin) were synthesized in our laboratory, rapeseed oil was purchased from market, and Crude oil was obtained from the Northern China Oil Field.

2.2. Preparation of Al_2O_3 sheet and smooth hydrophobic glass

The anodized aluminum sheets were prepared according to our previous report [26]. A cleaned Al sheet was firstly treated in 0.06 M Na_2SO_4 solution at 4 V bias at room temperature for 3 h, and then anodized at high field with constant current (325 mA cm^{-2}) to form nanostructures. At last, the anodized aluminum sheet was modified with 1H, 1H, 2H, 2H-perfluorooctyltrichlorosilane. A planar glass was ultrasonically cleaned in acetone and ethanol for 20 min to wipe off oil contamination, then irradiated with oxygen plasma for 2 min. The glass was soaked in 0.5% 1H, 1H, 2H, 2H-perfluorooctyltrichlorosilane solution for 2 h to hydrophobic modification.

2.3. The adhesive force measurement

The adhesive force was measured using a high-sensitivity micro-balance system (Dataphysics DCAT11, Germany). The liquid droplets of 5 μL suspended on a hydrophobic metal ring were approached and retracted from the sample surface at a constant speed of 0.01 mm/s at ambient environment. The droplet started to move away from the sample surface once contacted, and the balance force would gradually increase, and reach the maximum before the droplet broke away from the surface. The peak data recorded in the force–distance curve were taken as the break point adhesive force.

2.4. Contact angle measurements

The static oils contact angles of anodized aluminum sheet were measured using the contact angle goniometry (DSA100, Kruss) under ambient laboratory conditions. A droplet of 5 μL oil samples was utilized for all measurements with three replicate measurements for each specimen.

2.5. Slip measurement

The boundary shear strength was measured through torque measurement with a commercial rheometer (HAKKE, RS6000, Germany), and the operational torque range is between 0.2 mN m and 200 mN m with angular velocity between 10^{-7} and 1500 rpm. In rheology experiment, a stainless steel clamp with a diameter of 35 mm was used as the counter reference plate in a plate-to-plate configuration. The temperature was set by a Peltier plate at 20 ± 0.10 °C. The distance between the clamp and omniphobic surface was accurately controlled. Liquids that possess different surface tensions were injected into the gap by an accurate syringe. The clamp was driven with a certain angular velocity. The torque applied to the rotating clamp was measured over various shear rates. At each shear rate, the average torque over 30 s was recorded. The mathematical relation between the slip length and torque was derived in the previous study [25] on the assumption that a slip existed on the surface and was used to calculate the slip length from the measured torque in this study.

2.6. Morphology characterization

Scanning electron microscope (SEM) images were obtained on a JSM-6701F field emission scanning electron microscope (FE-SEM) at 5–10 kV.

3. Results and discussion

The morphology of anodized aluminum sheet after the first step of anodization at a low electric field and after the second step of anodization at a high electric field is shown in Fig. 2a–d. The micro-sized random terrace-shape structures were formed after the first step electrochemical etching. The distance between two terrace-shape structures ranges from ~5 μm to ~20 μm. After the second anodizing, the nano-wires about ~100 nm appeared on the terrace-shape structure. The formation mechanism of this feature was discussed in previous articles [26,27]. Because of the mi-